ACADEMIC PRESS

Available online at www.sciencedirect.com
SCIENCE DIRECT®

Journal of Catalysis 216 (2003) 505–516

JOURNAL OF CATALYSIS

www.elsevier.com/locate/jcat

The design and development of highly reactive titanium oxide photocatalysts operating under visible light irradiation

Masakazu Anpo * and Masato Takeuchi

Department of Applied Chemistry, Graduate School of Engineering, Osaka Prefecture University, 1-1, Gakuen-cho, Sakai, Osaka 599-8531, Japan

Received 24 July 2002; revised 17 October 2002; accepted 8 November 2002

Abstract

This review deals with the preparation of highly reactive titanium oxide photocatalysts and the clarification of the active sites as well as the detection of the reaction intermediates at the molecular level. Furthermore, we discuss the advancement of photofunctional systems and processes that can utilize visible and/or solar light. The photocatalytic reactivity of semiconducting TiO_2 powder was found to be dramatically enhanced by the loading of small amounts of Pt, which work to enhance the charge separation of the electrons and holes generated by light irradiation. Highly dispersed titanium oxide species prepared within zeolite frameworks or silica matrices showed unique photocatalytic performance much higher than that of conventional semiconducting TiO_2 photocatalysts. The potential for the effective utilization and conversion of solar energy makes research into the modification of the electronic properties of TiO_2 photocatalysts by such methods as advanced metal ion implantation to produce photocatalysts which are able to absorb and operate efficiently even under visible light irradiation one of the most important fields in photocatalysis research. This modification process can be applied not only to semiconducting TiO_2 photocatalysts but also to TiO_2 thin film photocatalysts, as well as titanium oxide photocatalysts highly dispersed within zeolite frameworks. Significantly, a new alternative method for directly preparing such visible-light-responsive TiO_2 thin film photocatalysts has been successfully developed by applying a RF magnetron sputtering deposition method.

1. Introduction

Since the discovery of the effect of photosensitization of the TiO_2 electrode on the electrolysis of water into H_2 and O_2 by Honda and Fujishima in 1972 [1], photocatalysis by TiO_2 semiconductors has received much attention and been widely studied, with the final aim of efficiently converting solar light energy into useful chemical energy [2–14]. The effective utilization of clean, safe, and abundant solar energy will lead to promising solutions not only for energy issues due to the exhaustion of natural energy sources but also for the many problems caused by environmental pollution. Fine TiO_2 semiconductor nanoparticles are ideal photocatalysts due to their chemical stability, nontoxicity, and high photocatalytic reactivity in the elimination of pollutants in air and water. TiO_2 semiconductor photocatalysts have the potential to oxidize a wide range of organic compounds, including chlorinated organic compounds, such as dioxins, into harmless compounds such as CO_2 and H_2O by irradiation with UV light [15–25]. UV light excites the electrons from the valence band to the conduction band of the TiO_2, leaving holes in the valence band. These electrons and holes can then initiate redox reactions with molecular species adsorbed on the surfaces of the catalysts.

A thorough and meticulous understanding of the photocatalytic processes will be necessary for the development and design of highly reactive photocatalysts, especially since such systems are to be applied to dilute concentrations of toxic reactants in the atmosphere and water on a huge global scale. The preparation of well-defined photocatalysts is necessary in order to identify and clarify the chemical features of the photoformed electrons and holes, to detect the reaction intermediate species and their dynamics, and to elucidate the reaction mechanisms at the molecular level, which in turn would necessitate a detailed and comprehensive investigation of the photogenerated active sites and the local structures [26–41].

We have conducted detailed studies of the characterization of various photocatalysts using a number of molecu-

* Corresponding author.
E-mail address: anpo@ok.chem.osakafu-u.ac.jp (M. Anpo).

0021-9517/03/$ – see front matter
doi:10.1016/S0021-9517(02)00104-5

lar spectroscopies in order to realize two main objectives: (i) the improvement of the photocatalytic reactivity [42–81] and (ii) the design and development of photocatalysts which are able to absorb and work under visible light irradiation [82–103].

Photocatalytic reactions on semiconducting TiO_2 photocatalysts were shown to be remarkably enhanced by the addition of small amounts of noble metals such as Pt. Such an enhancement in the photocatalytic reactivity has been explained in terms of a photoelectrochemical mechanism in which the electrons generated by UV irradiation of the TiO_2 semiconductor quickly transfer to the Pt particles loaded on the TiO_2 surface. These Pt particles work to effectively enhance the charge separation of the electrons and holes, resulting in marked improvement in photocatalytic performance. Recent time-resolved spectroscopic investigations clearly indicate the important role of Pt particles in the dynamics of such photoformed charge carriers [69,74–76].

Studies have also been carried out on extremely small TiO_2 powders as well as on various binary oxides [42,44, 47–56]. In particular, we have found that nanosized semiconducting TiO_2 particles of less than 10 nm show significant enhancement in photocatalytic reactivity, which can be attributed to the quantum size effect [44,49–53]. This phenomenon is due to electronic modification of the photocatalysts as well as the close existence of the photoformed electron and hole pairs and their efficient contribution to the reaction, resulting in a performance much enhanced over that of semiconducting TiO_2 powders. These findings have provided us with new insights into photocatalysts such as highly dispersed titanium oxide. Significantly, the application of an anchoring method makes possible the preparation of molecular and/or cluster-sized photocatalysts on various supports. Along these lines, highly dispersed titanium oxide species incorporated within the cavities or frameworks of zeolites are of great interest due to their unique local structure, such as their four-fold coordinated titanium oxide species, and photocatalytic properties significantly more efficient than those of semiconducting TiO_2 powders.

Photocatalytic systems in which various photosensitizing dyes are adsorbed and/or supported on semiconducting photocatalysts have also been widely investigated [104–119]. In these systems, the dyes absorb visible light to form electronically excited states and from these excited states, electrons are injected into the conduction bands of semiconductors, producing photosensitized photocatalysts which are able to work under visible light irradiation. However, these photosensitizing dyes are not thermally stable. Although numerous investigations have been carried out into visible-light-responsive photocatalysts by adding small amounts of such components as cations and metal oxides, no significant results could be obtained and these initial trials were found to have many limitations [120–124].

2. Design of highly efficient TiO_2 semiconductor photocatalysts

2.1. Pt loading on semiconducting TiO_2 photocatalysts

The photocatalytic reactivity of semiconducting TiO_2 is remarkably enhanced by the addition of small amounts of noble metals such as Pt or Rh; this is explained by the quick transfer of photogenerated electrons in TiO_2 semiconductors to the loaded metal particles, resulting in a decrease in electron–hole recombination, as well as in efficient charge separation. Although many studies have been carried out, there have been few direct investigations clarifying the effects of metal loading on the primary processes involved in photocatalytic reactions in solid–gas systems.

We have found that UV light irradiation of TiO_2 photocatalysts in the presence of sufficient amounts of water to form a monolayer on the surface (wet TiO_2 surface) in the presence of unsaturated hydrocarbons such as alkenes and alkynes led to the formation of alkanes by a hydrogenation reaction, accompanied by the fission of the carbon–carbon bond of the reactant molecules (hereafter referred to as photohydrogenolysis). Alkanes formed without the fission of such a carbon–carbon bond (hereafter referred to as photohydrogenation) were observed as minor products. In addition to the formation of these saturated hydrocarbons, the formation of oxygen-containing compounds such as CH_3CHO, CO, and CO_2 could also be detected [42,43,49].

Changes in the product yields depended on the amount of water remaining on the TiO_2 surface and also on the water pressure. We also observed D-atom-containing products in the photocatalytic hydrogenation reaction of unsaturated hydrocarbons with D_2O instead of H_2O. Therefore, we could conclude that the nondissociated water molecules adsorbed on the TiO_2 surface, not the surface hydroxyl groups, play an important role in this photocatalytic hydrogenolysis [43,46]. The Pt-loaded TiO_2 photocatalyst was found to mainly catalyze hydrogenation to form C_3H_8 without carbon–carbon bond fission, while unloaded TiO_2 photocatalyst was found to mainly catalyze hydrogenolysis and lead to the formation of C_2H_6 and CH_4.

Fig. 1 shows the growth of ESR signals attributed to Ti^{3+} which were generated on Pt-loaded TiO_2 and unloaded TiO_2 photocatalysts under UV light irradiation. The signal intensity of Ti^{3+} of the unloaded TiO_2 was found to increase linearly with the UV light irradiation time, while on the other hand, few changes in the signal intensity could be observed with Pt-loaded TiO_2. The Ti^{3+} site is expected to arise from the Ti^{4+} site at which the photogenerated electrons are trapped. These results clearly indicate that photogenerated electrons in the Pt-loaded TiO_2 quickly transfer from TiO_2 to Pt particles, so that few Ti^{3+} sites could be observed. These trapped electrons on the Pt particles enhance the reduction of protons to form atomic hydrogen ($H^+ + e^- \rightarrow H$), which catalyzes the photocatalytic hydrogenation caused by the effect of Pt loading.

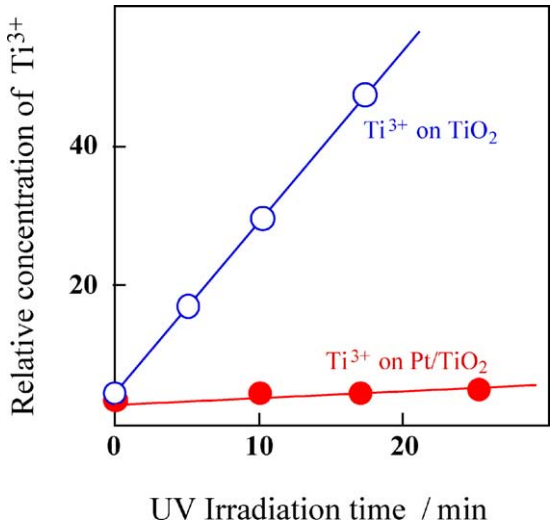

Fig. 1. Growth of the ESR signal intensity of the photoformed Ti^{3+} active site on Pt-loaded and unloaded on TiO_2 catalysts (recorded at 77 K).

From these findings, we have proposed the following mechanisms behind the observed photocatalytic reactions on unloaded TiO_2 and Pt-loaded TiO_2 catalysts:

(i) In the case of unloaded TiO_2 photocatalysts, UV light irradiation of the TiO_2 catalysts generates electron–hole pairs, which can be represented as localized electrons (Ti^{3+}) and holes (O^- (lattice) and/or ·OH radicals). Some of these electron–hole pairs disappeared by recombination on bulk TiO_2, while other electrons and holes diffused to the surface of the TiO_2 catalysts to react with various hydrocarbons, which led to photocatalytic reactions such as hydrogenolysis and the formation of oxygen-containing organic compounds [42,43,46,49,56,60].

(ii) In the case of Pt-loaded TiO_2 photocatalysts, the photogenerated electrons quickly transfer from TiO_2 to Pt particles and the holes remain on the TiO_2, resulting in charge separation of the photoformed electron–hole pairs with good efficiency. As a result, the reduction by photoformed electrons occurred on the Pt particles and the oxidation by photoformed holes on TiO_2, leading to photoelectrochemical reactions such as hydrogenation and oxidation. We have found that in TiO_2 photocatalysts having rather large particle sizes, these photoelectrochemical reactions are predominant and accompanied by a decrease in the contribution of the photocatalytic reactions.

Time-resolved spectroscopic experiments with photocatalytic systems provide more direct and detailed information on the dynamics of the photoformed charge carriers, charge separation and/or recombination, and charge transfer processes with high time resolution. For examples, Figs. 2A and 2B show the transient absorption spectra of the Ti^{3+} species generated by electron trapping, giving an absorption band at around 500–650 nm and the temporal profile of its absorption of TiO_2 (P-25) excited by a femtosecond laser pulse (390 nm) in a vacuum, respectively [69,74–76].

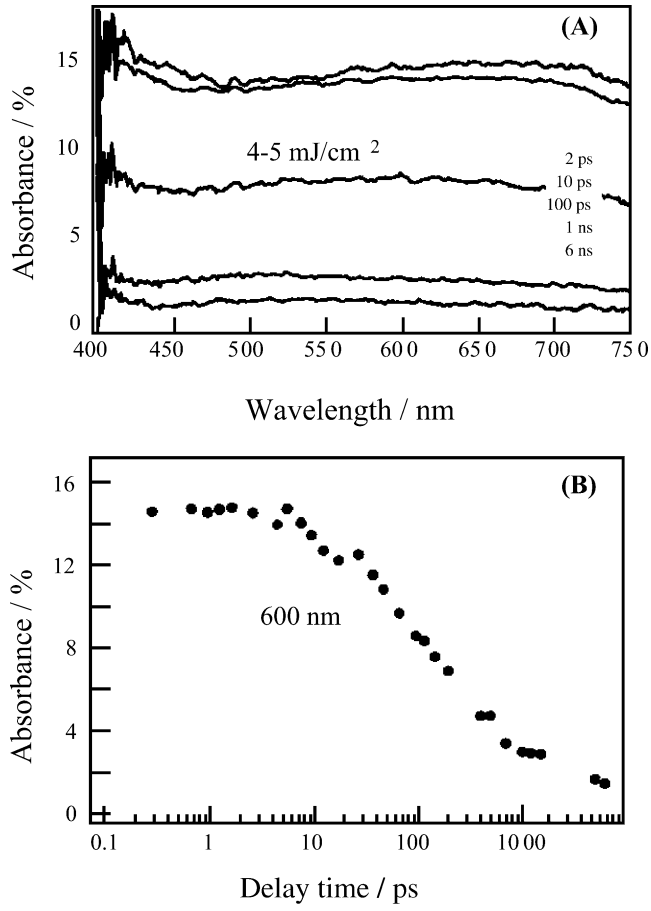

Fig. 2. Transient absorption spectra (A) and temporal profile of the transient absorption (B) of P-25 (Degussa) in a vacuum excited by a femtosecond laser pulse (390 nm).

2.2. Quantum size effect on nanosized photocatalysts

Table 1 shows the results of the photocatalytic hydrogenation of methylacetylene (C_3H_4) with H_2O on rutile-type TiO_2 catalysts having different particle sizes, together with BET surface areas, wavelengths at the adsorption edge positions, and the degree of blue shift of the band gap compared with that of the bulk TiO_2 catalyst. As shown in Table 1, we found that for both rutile and anatase type TiO_2 photocatalysts, the degree of blue shift in the absorption increased as the particle size of the catalysts decreased. In particular, for TiO_2 photocatalysts with a particle size less than 100 Å, a large shift to shorter wavelength regions was observed for both catalysts, resulting in an increase in the quantum yields, though the BET surface area increased in a uniform manner when the particle size of the catalysts decreased [49].

As already mentioned above, Pt-loaded TiO_2 photocatalysts were found to mainly catalyze the photocatalytic hydrogenation of C_3H_4 with H_2O to form hydrogenation products (i.e., C_3H_8) without carbon–carbon bond fission. On the other hand, unloaded TiO_2 photocatalysts catalyzed the hydrogenolysis reaction to mainly produce CH_4, C_2H_6, and oxygen-containing products. Improvements in the quantum

Table 1
Effect of Pt loading on the photocatalytic hydrogenation of methylacetylene (C_3H_4) by H_2O on rutile-type TiO_2 catalysts having various particle sizes (photocatalytic reaction was carried out at 300 K)

TiO_2 particle size (Å)	Pt content (wt%)	BET surface area (m^2/g)	Wavelength at band gap position (nm)	Magnitude of the shift at band gap (eV)	Photohydrogenation products (10^{-8} mol/g-cat h)		
					CH_4	C_2H_6	C_3H_8
55	0.0	533	398.0	0.0934	60.2	290.0	1.1
	4.0				28.9	160.0	1540.1
120	0.0	120	401.5	0.067	9.1	42.2	0.16
	4.0				0.62	5.4	135.0
400	0.0	26	406.2	0.01	6.82	28.9	0.09
	4.0				trace	1.0	56.0
2000	0.0	4.0	410.4	0.000	1.9	10.2	0.04
	4.0				trace	0.24	23.8

yields of the photocatalytic reactions with decreased particle diameters were also observed in the case of Pt-loaded TiO_2 photocatalysts. These results, obtained from both unloaded and Pt-loaded TiO_2, were closely associated with the size quantum effect rather than physical properties such as surface areas, resulting in a significant modification of the energy level in the localized photoexcited state of the TiO_2 photocatalysts. In other words, as the particle size of the photocatalysts decreases, the ratio of the surface to the bulk increases. As a result, the photogenerated electron–hole pairs can easily and quickly diffuse to the surface of the catalysts to form the active sites at which the photocatalytic (redox) reactions are induced.

3. Design of highly dispersed titanium oxide photocatalysts

3.1. Highly dispersed titanium oxide species anchored on various supports

The results obtained from nanosized fine particle TiO_2 photocatalysts gave us the idea of using well-defined and highly dispersed titanium oxide species supported or anchored on inert supports. It is of special interest to investigate the photocatalytic reactivities of highly dispersed titanium oxide species on such supports as porous glass, silica, and zeolites, since highly dispersed metal oxides can undergo dramatic modifications in electronic and reactive properties, resulting in an enhancement of their photocatalytic reactivity and selectivity.

We have found that titanium oxides anchored onto silica glass by the chemical vapor deposition (CVD) method exhibited an intense pre-edge peak in the XANES region. The presence of such a sharp pre-edge peak clearly indicates that the titanium oxide species on the supports have a unique local structure in tetrahedral coordination. ESR measurements are also a powerful technique for investigating the local structure of titanium oxide species anchored on supports. After photoreduction of highly dispersed titanium oxide catalysts with H_2 at 77 K, an ESR signal attributed to the tetrahedrally coordinated Ti^{3+} ions could be observed, in good agreement with the results obtained from XAFS measurements [45,49].

Titanium oxide species anchored on silica glass also exhibited photoluminescence having a peak at around 480 nm when excited by UV light irradiation at around 260 nm. Only photocatalysts which exhibited a sharp pre-edge peak in the XANES spectra showed photoluminescence spectra at 77 K. From these results, the absorption and photoluminescence spectra of the highly dispersed titanium oxide species were attributed to the following charge transfer process and the reverse process of recombination of the correlated electron–hole pairs, respectively:

$$\left(Ti^{4+}\text{–}O^{2-}\right) \underset{h\upsilon'}{\overset{h\upsilon}{\rightleftarrows}} \left(Ti^{3+}\text{–}O^{-}\right)^{*}. \tag{1}$$

The addition of O_2 or NO molecules led to efficient quenching of the photoluminescence. The photoluminescence, as well as its efficient quenching upon the addition of O_2 or N_2O, clearly indicates that the emitting sites, as active sites, are highly dispersed on the support surface due to efficient interaction with these quencher molecules.

UV light irradiation of anchored photocatalysts in the presence of unsaturated hydrocarbons and water mainly produced hydrogenolysis products. The yield of the photocatalytic hydrogenolysis of C_3H_4 with H_2O was found to be in good agreement with the intensity of the photoluminescence spectra, indicating that the charge transfer excited state, i.e., $(Ti^{3+}\text{–}O^{-})^{*}$, plays an important role in the photocatalytic hydrogenolysis on such highly dispersed titanium oxide catalysts. The initial reaction rate over these anchored titanium oxide photocatalysts was determined to be about 2–3 orders of magnitude higher than that of the powdered TiO_2 photocatalysts [45].

3.2. Photocatalytic reactivity of titanium oxide species incorporated within zeolite frameworks [125–140]

As mentioned above, the highly dispersed titanium oxide species having four-fold coordination anchored onto the supports showed unique photocatalytic performance much

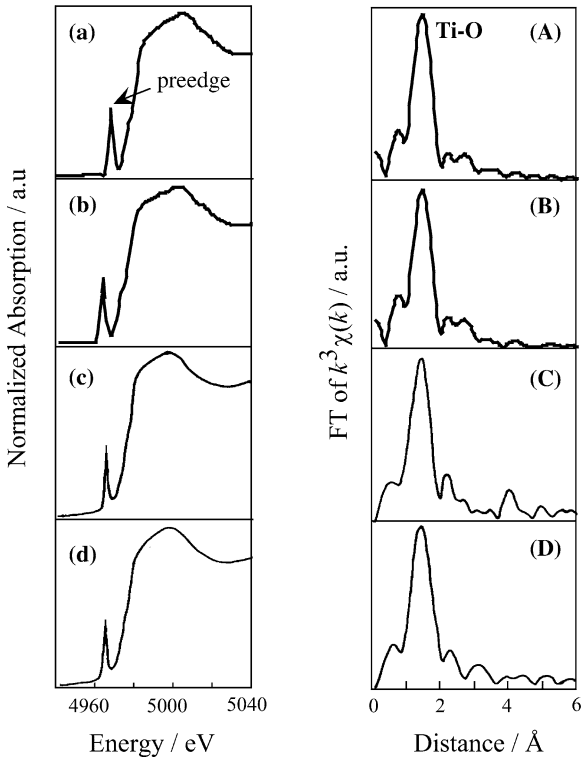

Fig. 3. Ti K-edge XANES (a–d) and Fourier transforms of EXAFS (A–D) spectra of the titanium oxide species incorporated within the various zeolite frameworks. (a, A) Ti-beta(OH), (b, B) Ti-beta(F), (c, C) Ti/HMS, (d, D) Ti/MCM-41.

higher than that of the powdered TiO_2 catalysts. Such highly dispersed titanium oxide species can be prepared within zeolite frameworks having tetrahedral coordination.

These highly dispersed molecular-sized titanium oxide species incorporated within zeolite frameworks showed unique photocatalytic performance, especially for the decomposition of NO into N_2 and O_2 [125–128] and the reduction of CO_2 with H_2O to form CH_3OH and CH_4 [129–140]. UV light irradiation of these catalysts in the presence of NO at 275 K was found to lead to the effective decomposition of NO to produce N_2 and O_2 with high selectivity, while the powdered bulk TiO_2 photocatalysts were found to decompose NO to produce mainly N_2O. It was found that the highly dispersed molecular-sized titanium oxide species prepared within the zeolite frameworks showed remarkable enhancement in selectivity for N_2 formation in the decomposition of NO, as well as reactivities much higher than those of semiconducting TiO_2 or the titanium oxide photocatalysts prepared by an impregnation method on silica and zeolite surfaces [61–65,128,133–140].

As shown in Fig. 3, the Ti K-edge XANES (left) and the Fourier transforms of EXAFS (right) of titanium oxides prepared within zeolite frameworks exhibit an intense preedge peak in the XANES region. The curve-fitting analysis of EXAFS oscillation clearly indicates that these catalysts consisted of four-fold coordinated Ti ions and involved only a well-defined and isolated tetrahedral titanium oxide species

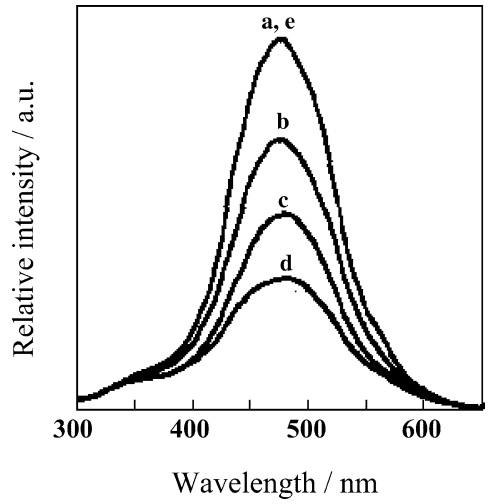

Fig. 4. The photoluminescence spectrum of the TS-2 catalyst at 77 K (a), and the effect of the addition of NO on it (b–d). NO pressure in Torr: (a) 0, (b) 0.05, (c) 0.1, (d) 0.3, (e) evacuation at 295 K after (d).

having a Ti–O bond distance of about 1.83 Å. On the other hand, catalysts prepared by an impregnation method were found to contain an aggregated octahedral TiO_2 species.

As shown in Fig. 4, these highly dispersed tetrahedral titanium oxide species incorporated within zeolite frameworks exhibit efficient photoluminescence at around 490 nm on excitation at around 250 nm. These results clearly show the presence of highly dispersed tetrahedrally coordinated titanium oxide species. Such a photoluminescence spectrum attributed to the four-fold coordinated titanium oxide species could be smoothly quenched by the addition of NO molecules, its extent depending on the amount of NO added. These findings indicate that the tetrahedrally coordinated titanium oxide species work as active sites accessible to the added NO and, furthermore, the added NO easily interacts with the charge transfer excited state, i.e., the $(Ti^{3+}–O^-)^*$ electron–hole pairs of the tetrahedral titanium oxide species. We have also proposed the reaction mechanism in Scheme 1 for the photocatalytic decomposition of NO over the highly dispersed titanium oxide species: electron transfer from the Ti^{3+} site, at which the photoformed electrons are trapped, into the anti-π^*-bonding orbital of NO, and simultaneous electron transfer from the π-bonding orbital of NO into the O^- site, at which the photoformed holes are trapped, occurs. Such simultaneous electron transfer leads to the direct decomposition of NO into N_2 and O_2 over the tetrahedrally coordinated titanium oxide photocatalyst.

3.3. Photocatalytic reactivity of titanium-oxide-based binary catalysts

Titanium-oxide-based binary catalysts combined with Al_2O_3 or SiO_2 can be easily prepared by the sol–gel method or a precipitation method [42–56]. The X-ray diffraction patterns of these binary-type oxides decreased in intensity and also broadened in peak width when the Ti content

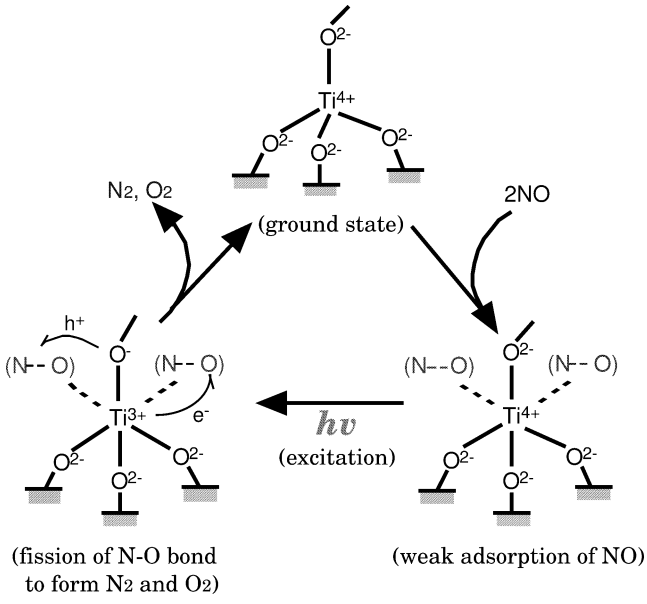

Scheme 1.

was decreased. These results indicate that the crystalline size of the titanium oxide particles in such binary oxide catalysts becomes smaller as the Ti content decreases. XAFS measurements of Ti/Si binary oxides having different Ti content revealed that binary oxides with lower Ti content (<10 wt%) mainly contain a tetrahedral TiO_4 unit with a Ti–O bond distance of about 1.83 Å within the SiO_2 matrices, while binary oxides having higher Ti content (>50 wt%) mainly consist of aggregated fine TiO_2 nanoparticles.

With Ti/Si binary oxide catalysts, a characteristic photoluminescence was observed at 490 nm upon excitation by UV light of around 260 nm. As mentioned above, this absorption and photoluminescence can be attributed to the charge transfer process and its reverse radiative deactivation from the excited state of the titanium oxide species, respectively. The peak positions of the photoluminescence were also observed to shift slightly toward shorter wavelength regions as the Ti content of the catalysts decreased. These results were in good agreement with the blue shifts in the absorption spectra.

These titanium-oxide-based binary catalysts were found to show efficient photocatalytic reactivity and selectivity for various photocatalytic reactions such as the hydrogenolysis reaction of unsaturated hydrocarbons with water, the decomposition of NO into N_2 and O_2, and the reduction of CO_2 with H_2O, as well as the oxidation of organic compounds in water. When the Ti content of these binary oxide catalysts decreased, the selectivity for N_2 formation in the photocatalytic decomposition of NO increased. We observed a good relationship between the intensity of photoluminescence and the yield of the photocatalytic reaction. Thus, the highly dispersed 4-coordinated titanium oxide species, showing efficient photoluminescence, play an important role in the photocatalytic decomposition of NO into N_2 and O_2 with high reactivity and selectivity.

3.4. Photocatalytic reduction of CO_2 by H_2O using titanium oxide incorporated within zeolites (Ti/zeolites) [129–140]

The development of efficient photocatalytic systems which are able to reduce CO_2 with H_2O into chemically valuable compounds such as CH_3OH or CH_4 is a challenging goal in research on environmentally friendly catalysts. We have found that highly dispersed tetrahedrally coordinated titanium oxide species within zeolite frameworks, when compared with bulk semiconducting TiO_2 catalysts, exhibit high and unique photocatalytic reactivity for the reduction of CO_2 with H_2O.

As mentioned above, titanium oxides incorporated within various zeolite frameworks contain isolated four-fold coordinated titanium oxide species having a Ti–O bond distance of about 1.83 Å. These Ti-containing zeolite catalysts exhibited a photoluminescence spectrum at around 480–490 nm by excitation at around 220–260 nm. The addition of H_2O or CO_2 molecules onto the Ti/zeolite catalysts led to efficient quenching of the photoluminescence as well as shortening of the lifetime of the charge transfer excited state, its extent depending on the amount of those gases added. Such efficient quenching of the photoluminescence with H_2O or CO_2 molecules suggests not only that four-fold coordinated titanium oxide species locate at positions accessible to these small molecules but also that they interact with these titanium oxides in both their ground and excited states. In fact, UV irradiation of the Ti/zeolite catalysts in the presence of a mixture of CO_2 and H_2O led to the photocatalytic reduction of CO_2 to form CH_3OH and CH_4 as major products as well as CO, O_2, C_2H_4, and C_2H_6 as minor products in the gas phase at 323 K, while the yields of these photoformed products increased with good linearity against the UV irradiation time. These results clearly indicate that highly dispersed tetrahedrally coordinated titanium oxide species exhibit high selectivity as well as efficiency for CH_3OH formation in the photocatalytic reduction of CO_2 with H_2O, as compared with bulk TiO_2 having an octahedral coordination.

Fig. 5 shows the relationship between the coordination number of the titanium oxide species of Ti/zeolite catalysts obtained from XAFS analyses and the selectivity for the formation of CH_3OH in the photocatalytic reduction of CO_2 with H_2O on various Ti/zeolite catalysts. The clear dependence of the selectivity for the formation of CH_3OH in the photocatalytic reduction of CO_2 with H_2O on the coordination numbers of the titanium oxide species of the catalysts can be observed; i.e., the lower the coordination number of the titanium oxide species, the higher the selectivity for the CH_3OH formation. Bulk TiO_2 semiconducting photocatalysts did not show any reactivity for the formation of CH_3OH from CO_2 and H_2O. From these results, it can be proposed that the highly efficient and selective photocatalytic reduction of CO_2 into CH_3OH by H_2O can be achieved using Ti/zeolite catalysts involving highly dispersed four-fold co-

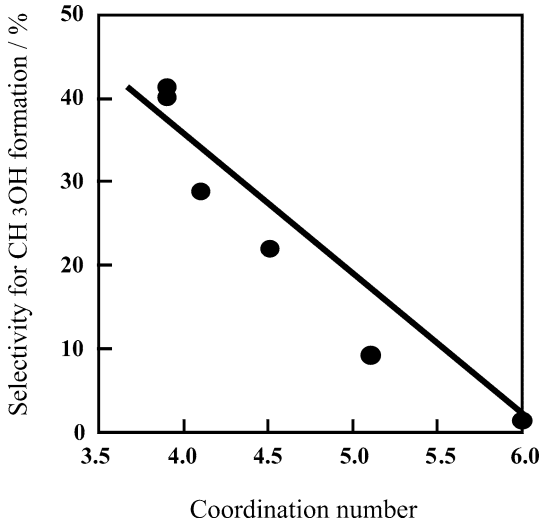

Fig. 5. The relationship between the selectivity of CH_3OH formation in the photocatalytic reduction of CO_2 with H_2O and the coordination number of titanium oxide species determined by the XAFS investigation.

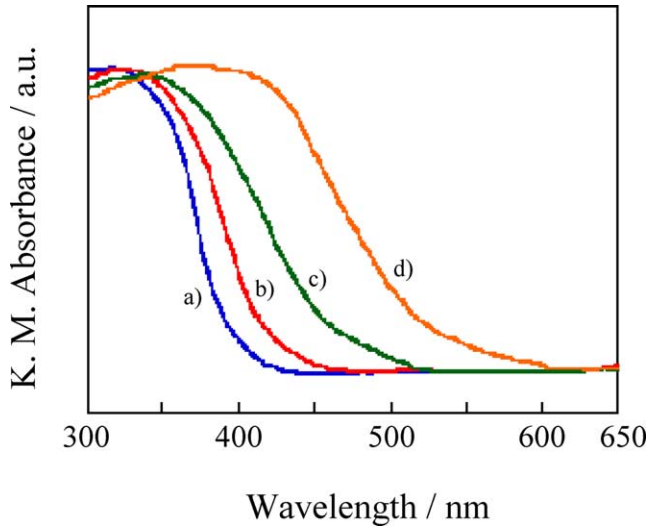

Fig. 6. The UV–vis absorption spectra of TiO_2(a) and Cr ion-implanted TiO_2 photocatalysts (b–d). The amount of implanted Cr ions (μmol/g); (a) 0, (b) 0.22, (c) 0.66, (d) 1.3.

ordinated titanium oxides in their frameworks as the active species.

4. Design and development of "second-generation TiO_2 photocatalysts" which can operate under visible light

4.1. Modification of the electronic state of TiO_2 by applying an advanced metal ion implantation method [82–103]

There are no limits to the possibilities and applications of photocatalytic systems for the purification of polluted air and water as well as safe conversion of solar light energy into chemical energy. However, TiO_2 semiconductors have a relatively large band gap of 3.2 eV, corresponding to wavelengths shorter than 388 nm. In other words, TiO_2 in itself can make use of only 3–4% of the solar energy that reaches the earth, necessitating a UV light source for its use as a photocatalyst. From this viewpoint, TiO_2 photocatalysts which can operate efficiently under both UV and visible light irradiation would be the ideal for practical and widespread use.

The metal-ion-implantation method was applied to modify the electronic properties of bulk TiO_2 photocatalysts by bombarding them with high-energy metal ions, and it was discovered that metal-ion implantation with various transition-metal ions such as V, Cr, Mn, Fe, and Ni accelerated by high voltage makes possible a large shift in the absorption band of the titanium oxide catalysts toward the visible light region, with differing levels of effectiveness. However, Ar-, Mg-, or Ti-ion-implanted TiO_2 exhibited no shift in the absorption spectra, showing that the shift is not caused by the high-energy implantation process itself, but by some interaction of the transition metal ions with the TiO_2 catalyst. As can be seen in Figs. 6b–6d, the absorption band of the Cr-ion-implanted TiO_2 shifts smoothly towards the visible light region, the extent of the red shift depending on the amount and type of metal ions implanted, with the absorption maximum and minimum values always remaining constant. The order of the effectiveness in the red shift was found to be V > Cr > Mn > Fe > Ni. Such a shift allows the metal-ion-implanted titanium oxide to use solar irradiation more effectively, with efficiencies in the range 20–30%.

Furthermore, such red shifts in the absorption band of the metal-ion-implanted TiO_2 catalysts were observed for any kind of titanium oxide except amorphous types, the extent of the shift changing from sample to sample. It was also found that such shifts in the absorption band were observed only after the calcination of the metal-ion-implanted TiO_2 samples in O_2 at around 723–823 K. Therefore, the calcination under O_2 in combination with metal-ion implantation was found to be instrumental in the red shift of the absorption spectrum toward the visible light region. These results clearly show that shifts in the absorption band of the TiO_2 catalysts by metal-ion implantation are a general phenomenon and not a special feature of certain kinds of bulk TiO_2 catalysts.

Fig. 7 shows the absorption spectra of the TiO_2 catalysts impregnated or chemically doped with Cr ions in large amounts as compared with those for Cr-ion-implanted samples. The Cr-ion-doped catalysts show no shift in the absorption edge of TiO_2; however, a new absorption band appears at around 420 nm as a shoulder peak due to the formation of an impurity energy level within the band gap, its intensity increasing with the number of Cr ions chemically doped. These results indicate that the method of doping causes the electronic properties of the TiO_2 catalyst to be modified in completely different ways, thus confirming that only metal-ion-implanted TiO_2 catalysts show such shifts in the absorption band toward the visible light region, even with much lower amounts of the ions, as compared with those for the chemically doped systems.

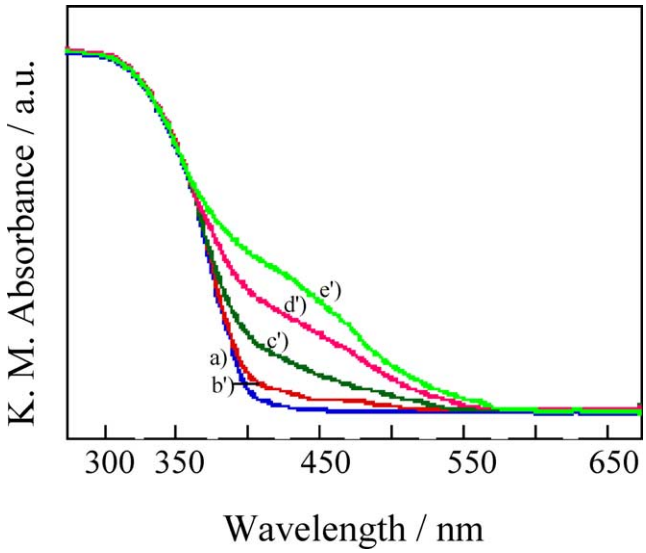

Fig. 7. The UV–vis absorption spectra of TiO_2 (a) and Cr ion-doped TiO_2 (b′–d′) photocatalysts prepared by an impregnation method. The amount of doped Cr ions (wt%): (a) 0, (b′) 0.01, (c′) 0.1, (d′) 0.5, (e′) 1. (0.1 wt% equals 4.9 μmol/g-TiO_2.)

With unimplanted original or chemically doped TiO_2 catalysts, the photocatalytic reaction does not proceed under visible light irradiation ($\lambda > 450$ nm). However, we have found that visible light irradiation of metal-ion-implanted TiO_2 catalysts can initiate various significant photocatalytic reactions. Visible light irradiation ($\lambda > 450$ nm) of the Cr-ion-implanted TiO_2 catalysts in the presence of NO at 275 K led to the decomposition of NO into N_2, O_2, and N_2O with good linearity against the light irradiation time. Under the same conditions of visible light irradiation, the unimplanted original pure TiO_2 catalyst did not exhibit any photocatalytic reactivity. The action spectrum for this reaction on the metal-ion-implanted TiO_2 catalysts was in good agreement with the absorption spectrum of the catalyst shown in Fig. 6, indicating that only metal-ion-implanted TiO_2 catalysts were effective for the photocatalytic decomposition reaction of NO under visible light irradiation. Thus, metal-ion-implanted TiO_2 catalysts were found to enable the absorption of visible light up to a wavelength of 400–600 nm and were also able to operate effectively as photocatalysts; hence their name, "second-generation TiO_2 photocatalysts."

It is important to emphasize that the photocatalytic reactivity of the metal-ion-implanted TiO_2 catalysts under UV light ($\lambda < 380$ nm) retained the same photocatalytic efficiency as the unimplanted original TiO_2 catalyst. When metal ions were chemically doped into the TiO_2 catalyst, the photocatalytic efficiency decreased dramatically under UV irradiation due to the quick recombination of the photoformed electrons and holes through the impurity energy levels formed by the doped metal ions within the band gap of the catalyst (in the case of Fig. 7). These results clearly suggest that physically implanted metal ions do not work as electron–hole recombination centers but only work to modify the electronic properties of the catalyst.

We have conducted various fieldwork experiments to test the photocatalytic reactivity of the newly developed TiO_2 catalysts under solar beam irradiation [102]. Under outdoor solar light irradiation at ordinary temperatures, the Cr- and V-ion-implanted TiO_2 catalysts showed several times higher photocatalytic reactivity for the decomposition of NO. It was also found that under solar light irradiation at ordinary temperatures, the V-ion-implanted TiO_2 catalysts showed several times higher photocatalytic reactivity for the hydrogenation of C_3H_4 with H_2O than the unimplanted original TiO_2 catalysts. These results, together with the results shown in Fig. 6, clearly show that by using second-generation titanium oxide photocatalysts developed by applying the metal-ion-implantation method, we are able to utilize visible and solar light energy more efficiently.

The relationship between the depth profiles of the metal ions implanted within TiO_2 catalysts having the same numbers of metal ions, such as V or Cr ions, and their photocatalytic efficiency under visible light irradiation was investigated. It was found that when the same numbers of metal ions were implanted into the deep bulk of the TiO_2 catalyst by applying high acceleration energies, the catalyst exhibited high photocatalytic efficiency under visible light irradiation. On the other hand, when a low acceleration energy was applied, the catalyst exhibited low photocatalytic efficiency under the same conditions of visible light irradiation.

It was also found that increasing the number of metal ions implanted into the deep bulk of the TiO_2 catalyst caused the photocatalytic efficiency of these catalysts to increase under visible light irradiation, passing through a maximum at around 6×10^{16} ions/cm^2, and then decreasing with a further increase in the number of metal ions implanted. The presence of ions at the near surfaces could be observed by ESCA measurement only on samples with a large number of metal ions implanted. Thus, these results clearly suggest that there are optimal conditions in the depth and number of metal ions implanted to achieve high photocatalytic reactivity under visible light irradiation.

The ESR spectra of the V-ion-implanted TiO_2 catalysts were measured before and after the calcination of the samples in O_2 at around 723–823 K. Distinct and characteristic reticular V^{4+} ions were detected only after calcination at around 723–823 K. It was found that when a shift in the absorption band toward the visible light region by V-ion implantation was observed, the presence of the reticular V^{4+} ions in those catalysts could be detected by ESR measurement. No such V ions having the same local structure or shifts in the absorption band have been observed with TiO_2 catalysts chemically doped with V ions.

The XANES and Fourier transforms of EXAFS oscillation of the TiO_2 catalysts chemically doped with Cr ions and also physically implanted with Cr ions were measured in order to clarify the local structures of these Cr ions. Results obtained from the analyses of XAFS spectra showed that in the TiO_2 catalysts chemically doped with Cr ions by an impregnation or sol–gel method, the ions were present as

aggregated Cr oxides having octahedral coordination similar to that of Cr_2O_3 and tetrahedral coordination similar to that of CrO_3, respectively. On the other hand, in the catalysts physically implanted with Cr ions, the ions were found to be present in a highly dispersed and isolated state in octahedral coordination, clearly suggesting that the Cr ions are incorporated into the lattice positions of the TiO_2 catalyst in place of the Ti ions.

These findings clearly show that modification of the electronic state of TiO_2 catalysts by metal-ion implantation is closely associated with the strong and long-distance interaction which arises between the TiO_2 and the metal ions implanted, and not with the formation of impurity energy levels within the band gap of the catalysts resulting from the formation of aggregated metal oxide clusters, which are often observed in the chemical doping of metal ions and/or oxides, as shown in Fig. 7.

Thus, the advanced metal-ion-implantation method has been successfully applied to modify the electronic property of the TiO_2 catalyst, enabling the absorption of visible light even longer than 550 nm and initiating various photocatalytic reactions effectively not only under UV but also under visible light irradiation. These results obtained in the photocatalytic reactions and various spectroscopic measurements of the catalysts clearly indicate that the implanted metal ions are highly dispersed within the deep bulk of the TiO_2 catalysts and work to modify the electronic nature of the catalysts without any changes in the chemical properties of the surfaces. These modifications were found to be closely associated with an improvement in the reactivity and sensitivity of the TiO_2 photocatalyst, enabling the TiO_2 catalyst to absorb and operate effectively not only under UV but also under visible light irradiation. As a result, under outdoor solar light irradiation at ordinary temperatures, transition-metal-ion-implanted TiO_2 catalysts showed several times higher photocatalytic efficiency than the unimplanted original TiO_2 catalysts.

4.2. *Visible-light-responsive Ti oxide/zeolite*

As mentioned previously, the XANES spectra of Ti/zeolite at the Ti *K*-edge clearly showed an intense pre-edge peak, which is related to the local structures surrounding the titanium oxide species in a tetrahedral symmetry [125–140]. The Fourier transforms of EXAFS spectra of the Ti/zeolite catalysts exhibited a strong peak at around 1.83 Å, which could be assigned to the neighboring oxygen atoms (a Ti–O bond), indicating the presence of an isolated titanium oxide species in these catalysts. By the curve-fitting analysis of the Fourier transforms of EXAFS spectra, it was found that titanium oxide species incorporated within the zeolite frameworks exist in tetrahedral coordination with a Ti–O bond distance of about 1.83 Å for various Ti/zeolite catalysts.

Fig. 8 shows the diffuse reflectance UV–vis absorption spectra of the V-ion-implanted Ti/HMS and Ti/MCM-41

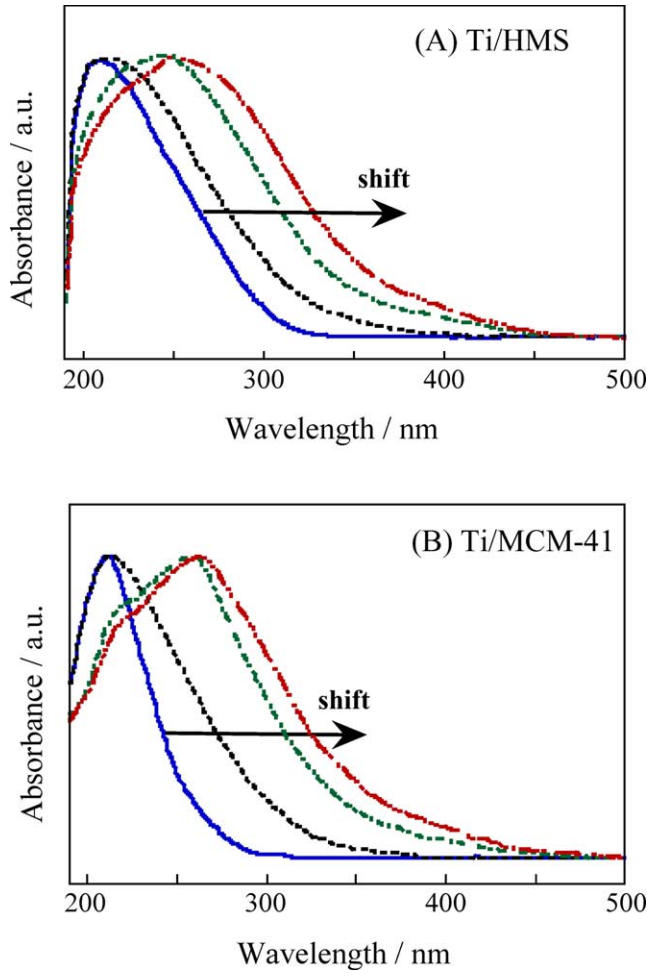

Fig. 8. The diffuse reflectance UV–vis absorption spectra of V-ion-implanted Ti/HMS (A) and Ti/MCM-41 (B). The amount of implanted V ions (μmol/g-cat): (a) 0, (b) 0.66, (c) 1.3, (d) 2.0.

catalysts. As mentioned above, the absorption spectra of these catalysts at around 200–260 nm can be attributed to the charge transfer absorption process, involving an electron transfer from the O^{2-} to the Ti^{4+} ion of the highly dispersed tetrahedrally coordinated TiO_4 unit of these catalysts. These absorption spectra shift smoothly toward the visible light region; the extent of the shift strongly depends on the amount of V ions implanted. These results clearly suggest that the interaction of implanted V ions with TiO_4 units leads to the modification of the electronic properties of the titanium oxide species within the zeolite frameworks.

The V *K*-edge FT-EXAFS spectra of Ti/HMS catalyst implanted with V ions indicated that the next neighbors of the V environment are not the same as vanadium-oxide-based catalysts (for example, V_2O_5) and suggested the formation of tetrahedral titanium oxides having a V–O–Ti bond instead of V–O–V linkages. These findings of V–O–Ti bridge structures in the V-ion-implanted Ti/HMS and also in Ti/MCM-41 catalysts do support the indication that is suggested by the red shift of absorption spectra of these catalysts.

We investigated the photocatalytic reactivity of these V-ion-implanted Ti/HMS and Ti/MCM-41 catalysts (also other Ti/zeolite catalysts such as Ti-beta zeolite) for the decomposition of NO into N_2 and O_2 under visible light irradiation ($\lambda > 420$ nm). As mentioned above, UV irradiation ($\lambda < 300$ nm) of Ti/HMS, Ti/MCM-41, and other Ti/zeolite catalysts in the presence of NO led to efficient decomposition of NO into N_2 and O_2. However, as expected from their absorption spectra, the unimplanted original Ti/HMS, Ti/MCM-41 and other Ti/zeolites did not catalyze the photocatalytic decomposition of NO under visible light irradiation, while visible light irradiation of the V-ion-implanted Ti/HMS, Ti/MCM-41, and other Ti/zeolites catalysts led to the decomposition of NO into N_2 and O_2, and the yield of the photoformed N_2 increased linearly with the irradiation time. These results clearly indicate that the photocatalytic decomposition of NO into N_2 and O_2proceeds on the V-ion-implanted Ti/HMS, Ti/MCM-41, and other Ti/zeolite catalysts even under visible light irradiation. It was also confirmed that the NO decomposition does not proceed at all under UV ($\lambda < 300$ nm) or visible light irradiation ($\lambda > 420$ nm) on the V-ion-implanted HMS, MCM-41, and other zeolites. These results clearly showed that the titanium oxide species in Ti/zeolite, Ti/HMS, and Ti/MCM-41 catalysts are present in tetrahedral coordination within the zeolite frameworks and that implanted V ions and highly dispersed Ti oxide species form the Ti–O–V linkage which leads to the modification of the electronic properties of tetrahedral Ti oxide species, enabling the absorption of visible light and operating as photocatalysts even under visible light irradiation ($\lambda > 420$ nm) with high photocatalytic efficiency for the decomposition of NO into N_2 and O_2.

4.3. Application of a RF magnetron sputtering deposition method to design TiO_2 thin film photocatalysts which operate under visible light irradiation

We have applied a RF magnetron (RF-MS) deposition method to prepare TiO_2 thin film photocatalysts using a TiO_2 plate as the sputtering target and Ar as the sputtering gas and successfully developed an alternative and more practical preparation method to create transparent TiO_2 thin films which can initiate various significant photocatalytic reactions effectively even under visible light irradiation [100,103]. Fig. 9 shows the UV–vis absorption (transmittance) spectra of TiO_2 thin films prepared by a RF-MS deposition method at different substrate temperatures. The thin films prepared at relatively low temperatures ($T <$ 473 K) exhibit high transparency and clear specific interference fringes in the visible light region, indicating that highly transparent and uniform thin films are formed on the substrate. The TiO_2 thin films prepared at relatively high temperatures ($T > 773$ K) exhibit efficient absorption in the visible light region, having maximum absorption with the thin film prepared at 873 K. These results clearly indicate that the TiO_2 thin films which can absorb visible light have

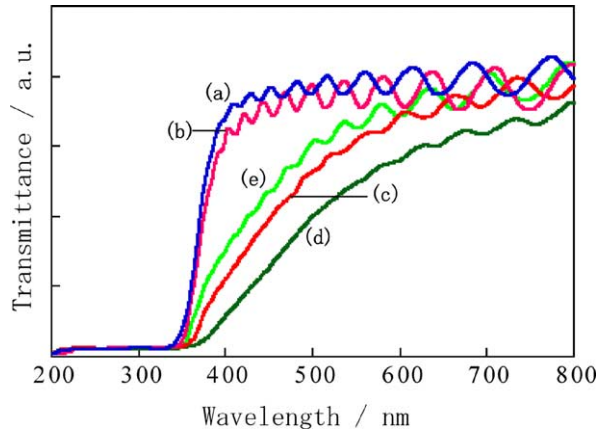

Fig. 9. The UV–vis absorption (transmittance) spectra of TiO_2 thin films prepared by a RF-MS deposition method. Preparation temperatures: (a) 373, (b) 473, (c) 673, (d) 873, (e) 973.

been successfully developed by applying a RF-MS deposition method. In fact, these TiO_2 thin films exhibited photocatalytic reactivities for various reactions such as the decomposition of NO, as well as the oxidation of acetaldehyde with O_2, not only under UV but also under visible light irradiation. Interestingly, recently, we have successfully carried out the photocatalytic decomposition of H_2O into H_2 and O_2 using newly developed visible-light responsive TiO_2 thin-film photocatalysts under visible light irradiation at wavelengths longer than 450 nm [141].

5. Conclusions

The preparations of nanosized TiO_2 particles, highly dispersed titanium oxide species within the zeolite cavities, titanium-oxide-based binary catalysts, second-generation TiO_2 photocatalysts which can operate under visible light irradiation by the advanced metal-ion implantation, and visible-light-responsive TiO_2 thin-film photocatalysts, as well as various characterizations of these photocatalysts at the molecular level, and also detailed investigations of various photocatalytic reactions on these photocatalysts have been summarized.

Special attention was focused on our research aims of achieving highly reactive photocatalysts, as well as realizing the efficient utilization of visible and/or solar light using a photocatalytic system. The direct detection of the intermediate reaction species at the molecular level provided important information to explain and clarify the reaction mechanisms behind the observed photocatalytic reactions as well as the electronic properties of the photocatalyst surface. Furthermore, the advanced metal-ion-implantation method and the RF-MS deposition method have opened the way to many innovative possibilities in the utilization of solar and/or visible light and the development of unique second-generation TiO_2 photocatalysts and visible-light-responsive molecular-sized titanium oxide species incorporated within the cavities and frameworks of zeolites and mesoporous

molecular sieves. Our findings showed that these visible-light-responsive titanium oxide catalysts can be considered promising candidates for use of solar energy to carry out environmentally friendly, clean, and safe reaction systems. A combination of fascinating and unique zeolite science and advanced ion engineering techniques will provide new approaches to the utilization of solar energy as an abundant and safe energy source, significantly addressing environmental pollution and hazards on a large global scale as well as the production of H_2 in the photocatalytic splitting of H_2O under solar irradiation.

References

[1] K. Honda, A. Fujishima, Nature 238 (1972) 37.
[2] T. Inoue, A. Fujishima, S. Konishi, K. Honda, Nature 277 (1979) 637.
[3] T. Kawai, T. Sakata, Chem. Phys. Lett. 72 (1980) 87.
[4] T. Kawai, T. Sakata, Nature 286 (1980) 31.
[5] G.N. Schrauzer, A.J. Bard, J. Am. Chem. Soc. 99 (1977) 7189.
[6] B. Kraeutler, A.J. Bard, J. Am. Chem. Soc. 100 (1978) 2239; J. Am. Chem. Soc. 100 (1978) 5985.
[7] A. Heller, A.A. Shalom, W.A. Bonner, B. Miller, J. Am. Chem. Soc. 104 (1982) 1688.
[8] M.A. Fox, Acc. Chem. Res. 16 (1983) 314.
[9] M.A. Fox, M.T. Dulay, Chem. Rev. 93 (1993) 341.
[10] S. Sato, J.M. White, J. Am. Chem. Soc. 102 (1980) 7206.
[11] H. Courbon, J.M. Herrmann, P. Pichat, J. Catal. 72 (1981) 129.
[12] M. Anpo, H. Yamashita, in: M. Anpo (Ed.), Surface Photochemistry, Wiley, London, 1996.
[13] M. Anpo, H. Yamashita, in: M. Schiavello (Ed.), Heterogeneous Catalysis, Willey, London, 1997.
[14] M. Anpo, in: G. Ertl, H. Knozinger, J. Weitkamp (Eds.), Handbook of Heterogeneous Catalysis, Wiley–VCH, Weinheim, 1997, and references therein.
[15] L.P. Childs, D.F. Ollis, J. Catal. 66 (1980) 383.
[16] A.L. Pruden, D.F. Ollis, J. Catal. 82 (1983) 404.
[17] I. Ait-Ichou, M. Formenti, B. Pommier, S.J. Teichner, J. Catal. 91 (1985) 193.
[18] S.A. Larson, J.A. Widegren, J.L. Falconer, J. Catal. 157 (1995) 611.
[19] J.L. Falconer, K.A. Magrini-Bair, J. Catal. 179 (1998) 171.
[20] M.D. Driessen, V.H. Grassian, J. Phys. Chem. B 102 (1998) 1418.
[21] D. Brinkley, T. Engel, J. Phys. Chem. B 104 (2000) 9836.
[22] M.C. Blount, J.L. Falconer, J. Catal. 200 (2001) 21.
[23] T. Tatsuma, S. Tachibana, A. Fujishima, J. Phys. Chem. B 105 (2001) 6987.
[24] D.F. Ollis, H. Al-Ekabi (Eds.), Photocatalytic Purification and Treatment of Water and Air, Elsevier, Amsterdam, 1993.
[25] N. Serpone, E. Pelizzetti (Eds.), Photocatalysis–Fundamentals and Applications, Wiley, New York, 1989.
[26] G. Calzaferri (Ed.), Solar Energy Materials and Solar Cells, in: Proceedings of the 10th International Conference on Photochemical Transfer and Storage of Solar Energy, Elsevier, Amsterdam, 1995.
[27] M. Anpo, Surface Photochemistry, Wiley, Chichester, 1996.
[28] Y. Kubokawa, K. Honda, Y. Saito, Hikarishokubai [Photocatalysis], Asakura-shoten, Tokyo, 1988.
[29] M. Anpo (Ed.), Photofunctional Zeolites, NOVA, 2000.
[30] M. Anpo, S. Higashimoto, Stud. Surf. Sci. Catal. 135 (2001) 123.
[31] A. Corma, Chem. Rev. 97 (1997) 2373.
[32] T. Maschmeyer, F. Rey, G. Sankar, J.M. Thomas, Nature 378 (1995) 159.
[33] K.I. Zamaraev, J.M. Thomas, Adv. Catal. 41 (1996) 335.
[34] S. Bordiga, S. Coluccia, C. Lamberti, L. Marchese, F. Boscherini, F. Buffa, F. Genoni, G. Leofanti, G. Petrini, G. Vlaic, J. Phys. Chem. 98 (1994) 4125.
[35] L. Marchese, T. Maschmeyer, E. Gianotti, S. Coluccia, J.M. Thomas, J. Phys. Chem. B 101 (1997) 8836.
[36] C. Lamberti, S. Bordiga, D. Arduino, A. Zecchina, F. Geobaldo, G. Spano, F. Genoni, G. Petrini, A. Carati, F. Villain, G. Vlaic, J. Phys. Chem. B 102 (1998) 6382.
[37] M.S. Rigutto, H. Van Bekkum, Appl. Catal. 68 (1991) 297.
[38] G. Centi, S. Perathoner, F. Trifiró, A. Aboukais, C.F. Aïssi, M. Guelton, J. Phys. Chem. 96 (1992) 2617.
[39] S. Dzwigaj, M. Matsuoka, R. Franck, M. Anpo, M. Che, J. Phys. Chem. B 102 (1998) 6309.
[40] S. Dzwigaj, M. Matsuoka, M. Anpo, M. Che, J. Phys. Chem. B 104 (2000) 6012.
[41] H. Yamashita, K. Yoshizawa, M. Ariyuki, S. Higashimoto, M. Che, M. Anpo, J. Chem. Soc. Chem. Commun. (2001) 435.
[42] M. Anpo, N. Aikawa, S. Kodama, Y. Kubokawa, J. Phys. Chem. 84 (1984) 569;
C. Yun, M. Anpo, S. Kodama, Y. Kubokawa, J. Chem. Soc. Chem. Commun. (1980) 609.
[43] M. Anpo, N. Aikawa, Y. Kubokawa, J. Phys. Chem. 88 (1984) 3998.
[44] M. Anpo, T. Shima, Y. Kubokawa, Chem. Lett. (1985) 1799.
[45] M. Anpo, N. Aikawa, Y. Kubokawa, M. Che, C. Louis, E. Giamello, J. Phys. Chem. 89 (1985) 5017.
[46] M. Anpo, Y. Ichihashi, in: Proc. of the 15th International Congress on Catalysis, The Taniguchi Conference, Kobe, 1995, p. 39.
[47] S. Kodama, H. Nakaya, M. Anpo, Y. Kubokawa, Bull. Chem. Soc. Jpn. 58 (1985) 3645.
[48] M. Anpo, M. Yabuta, S. Kodama, Y. Kubokawa, Bull. Chem. Soc. Jpn. 59 (1986) 259.
[49] M. Anpo, T. Shima, S. Kodama, Y. Kubokawa, J. Phys. Chem. 91 (1987) 4305.
[50] M. Anpo, Y. Kubokawa, Rev. Chem. Intermed. 8 (1987) 105.
[51] M. Anpo, H. Nakaya, S. Kodama, Y. Kubokawa, K. Domen, T. Onishi, J. Phys. Chem. 90 (1988) 1633.
[52] M. Anpo, T. Kawamura, S. Kodama, K. Maruya, T. Onishi, J. Phys. Chem. 92 (1988) 438.
[53] M. Anpo, T. Shima, M. Che, Chem. Express 3 (1988) 403.
[54] H. Yamashita, S. Kawasaki, Y. Ichihashi, M. Harada, M. Takeuchi, M. Anpo, J. Phys. Chem. B 102 (1998) 5870.
[55] H. Yamashita, S. Kawasaki, Y. Ichihashi, M. Takeuchi, M. Harada, M. Anpo, Korean J. Chem. Eng. 15 (1998) 491.
[56] M. Anpo, K. Chiba, M.A. Fox, M. Che, Bull. Chem. Soc. Jpn. 64 (1991) 543.
[57] H. Yamashita, H. Nishiguchi, M. Anpo, M.A. Fox, Res. Chem. Intermed. 20 (1994) 815.
[58] M. Anpo, H. Yamashita, Y. Ichihashi, S. Ehara, J. Electroanal. Chem. 396 (1995) 21.
[59] H. Yamashita, Y. Ichihashi, M. Harada, G. Stewart, M.A. Fox, M. Anpo, J. Catal. 158 (1996) 97.
[60] M. Anpo, T. Shima, T. Fujii, M. Che, Chem. Lett. (1987) 65.
[61] M. Anpo, K. Chiba, J. Mol. Catal. 74 (1992) 207.
[62] M. Anpo, M. Tomonari, M.A. Fox, J. Phys. Chem. 93 (1989) 7300.
[63] H. Yamashita, Y. Ichihashi, M. Anpo, M. Hashimoto, C. Louis, M. Che, J. Phys. Chem. 100 (1996) 16041.
[64] S.G. Zhang, Y. Ichihashi, H. Yamashita, T. Tatsumi, M. Anpo, Chem. Lett. (1996) 895.
[65] H. Yamashita, M. Anpo, Surf. Sci. Jpn. 17 (1996) 30.
[66] M. Anpo, S.G. Zhang, H. Yamashita, in: Proceedings of the 11th International Congress on Catalysis, Baltimore, 1996, p. 941.
[67] M. Anpo, H. Yamashita, Y. Ichihashi, Y. Fujii, M. Honda, J. Phys. Chem. B 101 (1997) 2632.
[68] H. Yamashita, M. Honda, M. Harada, Y. Ichihashi, M. Anpo, J. Phys. Chem. B 102 (1998) 10707.
[69] A. Furube, T. Asahi, H. Masuhara, H. Yamashita, M. Anpo, J. Phys. Chem. B 103 (1999) 3120.
[70] D.R. Park, J.L. Zhang, K. Ikeue, H. Yamashita, M. Anpo, J. Catal. 185 (1999) 114.
[71] Y. Yoshida, M. Matsuoka, S.-C. Moon, H. Mametsuka, E. Suzuki, M. Anpo, Res. Chem. Intermed. 26 (2000) 567.

[72] H. Yamashita, M. Harada, A. Tanii, M. Honda, M. Takeuchi, Y. Ichihashi, M. Anpo, Stud. Surf. Sci. Catal. 130 (2000) 1931.
[73] S. Dohshi, M. Takeuchi, M. Anpo, J. Nanosci. Nanotechnol. 1 (2001) 337.
[74] H. Furube, T. Asahi, H. Masuhara, H. Yamashita, M. Anpo, Res. Chem. Intermed. 27 (2001) 177.
[75] H. Furube, T. Asahi, H. Masuhara, H. Yamashita, M. Anpo, Chem. Phys. Lett. 336 (2001) 424.
[76] A. Furube, T. Asahi, H. Masuhara, H. Yamashita, M. Anpo, Chem. Lett. (1997) 735.
[77] M. Takeuchi, M. Matsuoka, H. Yamashita, M. Anpo, J. Synchrotron Radiat. 8 (2001) 643.
[78] J. Zhang, Y. Hu, M. Matsuoka, H. Yamashita, M. Minagawa, H. Hidaka, M. Anpo, J. Phys. Chem. B 105 (2001) 8395.
[79] M. Ogawa, K. Ikeue, M. Anpo, Chem. Mater. 13 (2001) 2900.
[80] J. Zhang, M. Minagawa, M. Matsuoka, H. Yamashita, M. Anpo, Catal. Lett. 66 (2000) 241.
[81] J. Zhang, M. Minagawa, T. Ayusawa, S. Natarajan, H. Yamashita, M. Matsuoka, M. Anpo, J. Phys. Chem. B 104 (2000) 11501.
[82] Y. Ichihashi, H. Yamashita, M. Anpo, Kinou-Zairyou 16 (1996) 12.
[83] M. Anpo, H. Yamashita, Y. Ichihashi, Optronics 186 (1997) 161.
[84] M. Anpo, Catal. Survey Jpn. 1 (1997) 169.
[85] M. Anpo, Y. Ichihashi, M. Takeuchi, H. Yamashita, Res. Chem. Intermed. 24 (1998) 143.
[86] M. Anpo, Y. Ichihashi, M. Takeuchi, H. Yamashita, in: H. Hattori, K. Otsuka (Eds.), Sci. Tech. in Catal. 1998, Kodan-sha, Tokyo, 1999, p. 305.
[87] M. Anpo, M. Takeuchi, H. Yamashita, T. Hirao, N. Itoh, N. Iwamoto, in: Proc. Intern. Conf. “The 4th International Conference ECOMATERIAL”, Gifu, 1999, p. 333.
[88] M. Anpo, M. Che, Adv. Catal. 44 (1999) 119, and references therein.
[89] M. Anpo, Y. Ichihashi, M. Takeuchi, H. Yamashita, Stud. Surf. Sci. Catal. 121 (1999) 305, Proc. Tocat-3, Tokyo.
[90] M. Anpo, M. Takeuchi, S. Kishiguchi, H. Yamshita, Surf. Sci. Jpn. 20 (1999) 60.
[91] M. Anpo, H. Yamashita, S. Kanai, K. Sato, T. Fujimoto, US Patent 6,077,492, June 20, 2000.
[92] M. Takeuchi, H. Yamashita, M. Matsuoka, T. Hirao, N. Itoh, N. Iwamoto, M. Anpo, Catal. Lett. 66 (2000) 185.
[93] M. Takeuchi, H. Yamashita, M. Matsuoka, T. Hirao, N. Itoh, N. Iwamoto, M. Anpo, Catal. Lett. 67 (2000) 135.
[94] M. Anpo, in: Green Chemistry, Oxford University Press, Oxford, 2000, p. 1.
[95] M. Anpo, Pure Appl. Chem. IUPAC 72 (2000) 1265.
[96] M. Anpo, Stud. Surf. Sci. Catal. 130 (2000) 157.
[97] M. Anpo, S. Kishiguchi, Y. Ichihashi, M. Takeuchi, H. Yamashita, K. Ikeue, B. Morin, A. Davidson, M. Che, Res. Chem. Intermed. 27 (45) (2001) 459.
[98] M. Anpo, in: A. Corma, et al. (Eds.), 12th International Congress on Catalysis, in: Stud. Surf. Sci. Catal., Vol. 130, Elsevier, 2000, p. 157.
[99] M. Anpo, M. Takeuchi, Int. J. Photoenergy 3 (2001) 1.
[100] M. Takeuchi, M. Anpo, T. Hirao, N. Itoh, N. Iwamoto, Surf. Sci. Jpn. 22 (9) (2001) 561.
[101] H. Yamashita, M. Harada, J. Misaka, M. Takeuchi, Y. Ichihashi, F. Goto, M. Ishida, T. Sasaki, M. Anpo, J. Synchrotron Radiat. 8 (2001) 569.
[102] K. Takami, N. Segawa, H. Uehara, M. Anpo, Shokubai 41 (2002) 295.
[103] M. Anpo, M. Takeuchi, in: Handbook of Ion Engineering, 2002, p. 943.
[104] B. O’Regan, M. Gratzel, Nature 353 (1991) 737.
[105] K. Kalyanasundaram, M. Gratzel, Angew. Chem. Int. Ed. Eng. 18 (1979) 701.
[106] E. Borgarello, J. Kiwi, M. Gratzel, E. Pelizzetti, M. Visca, J. Am. Chem. Soc. 104 (1982) 2996.
[107] Y. Tachibana, J.E. Moser, M. Gratzel, D.R. Klug, J.R. Durrant, J. Phys. Chem. 100 (1996) 20056.
[108] W.D.K. Clark, N. Sutin, J. Am. Chem. Soc. 99 (1977) 4676.
[109] P.V. Kamat, M.A. Fox, Chem. Phys. Lett. 102 (1983) 379.
[110] K.R. Gopidas, P.V. Kamat, J. Phys. Chem. 93 (1989) 6428.
[111] C. Nasr, K. Vinodgopal, S. Hotchandani, A. Chattopadhyaya, P.V. Kamat, J. Phys. Chem. 100 (1996) 8436.
[112] L. Ziolkowski, K. Vinodgopal, P.V. Kamat, Langumuir 13 (1997) 3124.
[113] K. Murakoshi, G. Kano, Y. Wada, S. Yanagida, H. Miyazaki, M. Matsumoto, S. Murasawa, J. Electroanal. Chem. 396 (1995) 27.
[114] K. Tennakone, G.R.R.A. Humara, A.R. Kumarasinghe, K.G.U. Wijayantha, P.M. Sirimanne, Semiconduct. Sci. Technol. 10 (1995) 1689.
[115] M. Gratzel, J. Sol–Gel Sci. Technol. 22 (2001) 7.
[116] K. Hara, H. Sugihara, Y. Tachibana, A. Islam, M. Yanagida, K. Sayama, H. Arakawa, G. Fujihashi, T. Horiguchi, T. Kinoshita, Langmuir 17 (2001) 5992.
[117] A. Islam, H. Sugihara, K. Hara, L.P. Singh, R. Katoh, M. Yanagida, Y. Takahashi, S. Murata, H. Arakawa, J. Photochem. Photobiol. A Chem. 145 (2001) 135.
[118] K. Hara, H. Horiuchi, R. Katoh, L.P. Singh, H. Sugihara, K. Sayama, S. Murata, M. Tachiya, H. Arakawa, J. Phys. Chem. B 106 (2002) 374.
[119] K. Sayama, S. Tsukagoshi, K. Hara, T. Ohga, A. Shimpo, Y. Abe, S. Suga, H. Arakawa, J. Phys. Chem. B 106 (2002) 1363.
[120] A.K. Ghosh, H.P. Maruska, J. Electrochem. Soc. 124 (1977) 1516.
[121] E. Borgarello, J. Kiwi, M. Gratzel, E. Pelizetti, M. Visca, J. Am. Chem. Soc. 104 (1982) 2996.
[122] M.R. Hoffman, S.T. Martin, W. Choi, D.W. Bahnemann, Chem. Rev. 95 (1995) 69.
[123] J.M. Jerrmann, J. Disdier, P. Pichat, Chem. Phys. Lett. 108 (1984) 618.
[124] H.P. Maruska, A.K. Ghosh, Solar Energy Mater. 1 (1979) 237.
[125] M. Anpo, S.G. Zhang, S. Higashimoto, M. Matsuoka, H. Yamashita, Y. Ichihashi, Y. Matsumura, Y. Souma, J. Phys. Chem. B 103 (1999) 9295.
[126] S.G. Zhang, Y. Fujii, H. Yamashita, K. Koyano, T. Tatsumi, M. Anpo, Chem. Lett. (1997) 659.
[127] J. Zhang, M. Minagawa, M. Matsuoka, H. Yamashita, M. Anpo, Catal. Lett. 66 (2000) 241.
[128] J. Zhang, M. Matsuoka, H. Yamashita, M. Anpo, J. Synchrotron Radiat. 8 (2001) 637–639.
[129] M. Anpo, T. Suzuki, E. Giamello, M. Che, in: New Developments in Selective Oxidation, Elsevier, Amsterdam, 1990, p. 683.
[130] M. Anpo, M. Kondo, S. Coluccia, C. Louis, M. Che, J. Am. Chem. Soc. 111 (1989) 8791.
[131] S.G. Zhang, M. Ariyuki, H. Mishima, S. Higashimoto, H. Yamashita, M. Anpo, Micropor. Mesopor. Mater. 21 (1998) 621.
[132] S.G. Zhang, S. Higashimoto, H. Yamashita, M. Anpo, J. Phys. Chem. B 102 (1998) 5590.
[133] M. Anpo, H. Yamashita, Y. Fujii, Y. Ichihashi, S.G. Zhang, D.R. Park, S. Ehara, S.E. Park, J.S. Chang, J.W. Yoo, Stud. Surf. Sci. Catal. 114 (1998) 177.
[134] M. Anpo, H. Yamashita, K. Ikeue, Y. Fujii, S.G. Zhang, Y. Ichihashi, D.R. Park, Y. Suzuki, K. Koyano, T. Tatsumi, Catal. Today 44 (1998) 327.
[135] H. Yamashita, Y. Fujii, Y. Ichihashi, S.G. Zhang, K. Ikeue, D.R. Park, K. Koyano, T. Tatsumi, M. Anpo, Catal. Today 45 (1998) 221.
[136] K. Ikeue, H. Yamashita, M. Anpo, Chem. Lett. (1999) 1135.
[137] K. Ikeue, H. Mukai, H. Yamashita, S. Inagaki, M. Matsuoka, M. Anpo, J. Synchrotron Radiat. 8 (2001) 640.
[138] K. Ikeue, H. Yamashita, M. Anpo, J. Phys. Chem. B 105 (2001) 8350.
[139] K. Ikeue, H. Yamashita, T. Takewaki, M.E. Davis, M. Anpo, J. Synchrotron Rad. 8 (2001) 602.
[140] K. Ikeue, S. Nozaki, M. Ogawa, M. Anpo, Catal. Lett. 80 (2002) 111.
[141] M. Kitano, M. Matsuoka, M. Takeuchi, M. Anpo, unpublished data.